Article

JOURNAL OF COMPOSITE MATERIALS

Journal of Composite Materials
2019, Vol. 53(18) 2593–2605

DOI: 10.1177/0021998319834673
journals.sagepub.com/home/jcm
SAGE

Characterization and optimization of hybrid carbon–glass epoxy composites under combined loading

V Infante[1], JFA Madeira[1,2], Rui B Ruben[3], F Moleiro[1] and Sofia Teixeira de Freitas[4]

Abstract

This work is intended to characterize the mechanical behavior of hybrid carbon–glass composite plates under combined loading of bending and torsion, and to determine the optimal ply fiber orientations to minimize the maximum out-of-plane displacement under such loading conditions. Hybrid composite plates were manufactured with 10 plies each and different stacking sequences using hand lay-up, with carbon fiber and glass fiber reinforcements in an epoxy matrix. Two experimental setups (involving two distinct boundary conditions) are here considered to test the composite plates, both simulating combined loading of bending and torsion. Numerical simulations of the experimental tests were performed in ABAQUS® and validated with the experimental data. Using the ply fiber orientations as design variables, the hybrid composite plates were then optimized using global and local optimization using direct search (GLODS). The objective function of minimization of the maximum out-of-plane displacement is carried out through an interactive cycle between GLODS and ABAQUS®. Specimens of three optimized laminates were also manufactured for experimental validation. The optimization process contributed to improve the performance of the hybrid composite plates in more than 30% when compared to some non-optimized plates.

Keywords

Hybrid composites, carbon and glass fibers, finite element analysis, optimization

Introduction

Polymer matrix composites are becoming increasingly important in high-technology applications, particularly in the aeronautical industry. Aircraft designers typically look for high specific stiffness, high specific strength, low density, and reduced cost while selecting the material systems for different structural components. However, due to their characteristic high stiffness and strength, most of the composite materials, using single material reinforcements, have limited toughness values.

Hybrid composites may offer an effective solution for increasing the toughness of a composite material. By combining two fiber types in a single composite, one can take advantage of both fiber properties and try to minimize some of their disadvantages. The hybrid composites concept consist in combining fibers with high modulus and high specific strength, relatively brittle and generally expensive, with fibers with low modulus and lower specific strength, more ductile and frequently cheaper. Carbon fiber laminates are widely used in several applications due to their high specific modulus and strength. Nonetheless, the impact strength of these composites is generally lower than many metal alloys. Previous research has shown that an efficient method of increasing the tensile ultimate strain,[1] impact properties[2] as well as flexural strength properties[3,4] of carbon fiber composites is to add some percentage of low modulus fibers, such as glass fibers, both using

[1]LAETA, IDMEC, Instituto Superior Técnico, Universidade de Lisboa, Portugal
[2]Department of Mathematics, ISEL, IPL, Portugal
[3]CDRsp – ESTG – Polytechnic Institute of Leiria, Portugal
[4]Faculty of Aerospace Engineering, Delft University of Technology, Netherlands

Corresponding author:
Rui B Ruben, ESTG – Polytechnic Institute of Leiria, Campus 2 Morro do Lena – Alto do Vieiro, 2411-901 Leiria, Portugal.
Email: rui.ruben@ipleiria.pt

intra- or interply hybridization. With this hybridization, the carbon fiber can still provide the necessary stiffness, while the final composite material is cheaper and more damage tolerant due to the presence of the glass fibers. The final mechanical properties of the hybrid composite can be tailored by changing the stacking sequence of the plies (interply hybrid composites – different fiber materials along the stacking sequence) and the volume fraction of each fiber (intraply hybrid composite – different fiber material inside the plies).[5]

The impact performance of interply hybrid composites has been extensively reported by several works found in literature which concluded that hybrid carbon–glass epoxy composites show an improvement in damage tolerance and carrying capacity after impact in comparison with carbon/epoxy laminates with slight reduction of stiffness.[2,6–8] González et al.[9] further demonstrates that the stacking sequence of the carbon–glass hybrid composites has a significant influence on the failure mechanisms sequence, growth, and interactions during impact tests and compression after impact tests.

Under bending conditions, literature suggests that the best flexural properties of hybrid glass–carbon laminates are obtained when the carbon plies are positioned at the exterior.[10] The same study concludes that the tensile strength was insensitive to the relative position of the glass–carbon plies and an alternate glass–carbon stacking sequence favors compressive strength. Dong et al.[3] Dong and Davies[4] tested hybrid laminates under three-point bending and observed that the highest flexural strength is achieved when specimens contain 24% of glass fibers. These hybrid laminates show an increase of 8% and 3% when compared to the ones with full carbon and glass configurations, respectively. Simulation studies show much higher increases in flexural strength than the corresponding experiments. When looking to intraply hybrid laminates, literature shows that the fiber volume fraction has a significant influence on the flexural strength. Dong and Davies[11] claims that in general in order to improve flexural strength, the fiber volume fraction of glass/epoxy plies needs to be higher than that of carbon/epoxy plies.[12] Few studies were found in which an optimization of the stacking sequence was performed. Kalantari et al.[13,14] run multiobjective optimization analysis with several objectives such as flexural strength, weight, and costs. The results suggest that the hybridization of carbon fiber reinforced composites with glass fibers, and vice versa, not only improves the flexural strength but can also optimize the weight and cost of the composite structure.

Hybrid laminates can also be used for health monitoring purposes. Loading the hybrid composite in the fiber direction in tension will cause the more brittle fibers to fail before the more ductile fibers. Also, in a laminate with only carbon fiber reinforcements, the replacement of the middle plies by cheaper glass fibers can significantly reduce its cost, while the flexural properties remain almost unaffected.[15] The extensive work performed on characterizing the properties of fiber hybridization under tensile, flexural, and impact loading is reported in the comprehensive review of Swolfs et al.[15]

Optimization of composite materials in the field of design of ply orientation has drawn extensive attention over the past two decades.[16] Todoroki and Haftka[17] use the genetic algorithm (GA) to optimize ply orientation by considering the enforcement constraints to limit the number of continuous orientation plies. Toropov et al.[18] applied GA to optimize the weight and manufacturability of composite aircraft components. Zhu et al.[19] applied GA to a multiobjective linear variable weights to optimize the stacking sequence and ply thickness of carbon fiber composite struts. The advantage of using such heuristic algorithms is that there is no need to derive design sensitivity information and also the possibility of converging to a global optimum. Another class of methods that does not need any gradient information, but rather require only the value of the objective function, are the direct search methods.[20] The Direct MultiSearch (DMS)[21] is a direct search method for multiobjective optimization. In fact, it has been recently used by Araújo et al.[22] to find the optimal positioning of surface bonded sensors and actuators for damping maximization. It has also been used to solve the problem of minimum weight and maximum damping of viscoelastic sandwich plates by Madeira et al.[23,24] and to the design optimization of laminated composite plates with piezoelectric layers by Franco Correia et al.,[25] among other applications. Global and Local Optimization using Direct Search (GLODS) is a direct search method designed to deal with global optimization problems with a single objective function. This method has been used previously by Monte et al.[26] to optimize the carbon fibers orientation of composite plates in order to minimize their global out-of-plane displacement. The optimization process has been validated with experimental results. In this paper, GLODS is used to optimize a hybrid composite plate under combined loading of bending and torsion.

The works found in literature up to now on hybrid composites focus on their characterization and optimization under one single loading, such as isolated tensile, or isolated compression, or isolated bending. Nevertheless, in real composite structures such loading conditions are rare and a combined loading is often more realistic, for instance, the combined loading of bending and torsion that often occurs in wing skins of an aircraft. Therefore, it is considered essential for their applicability to investigate the properties of hybrid

composites under combined loading of bending and torsion. This paper aims exactly to fill in this gap of knowledge in the current state of the art and go one step further by optimizing the hybrid composite stacking sequence for combined loading conditions.

The main objective of this study is therefore to characterize the mechanical behavior of hybrid composite plates under combined loading of bending and torsion as well as to determine the optimal ply fiber orientations to minimize the maximum out-of-plane displacement under this loading condition.

Materials and specimens

The two fiber types used in hybrid composites are typically referred to as low-elongation (LE) and high-elongation (HE) fibers.[15] In the present work, the LE and HE fibers are high strength (HS) carbon fibers and E-glass fibers, respectively, and these can be combined in many different configurations. The different non-optimized specimens analyzed were produced using the most common ply fiber orientations of 0° and 90° with different stacking sequences.

The specimens were produced using the T700S carbon and E-glass reinforcements in an epoxy matrix resin. The matrix properties are presented in Table 1, in agreement with the supplier (Sicomin®) Technical Datasheet. Specifications for the fabrics and filaments used as reinforcements are presented in Table 2. And in Table 3, the fiber volume fraction of hybrid composites and ply and laminate thickness are presented.

Five hybrid composite plates were produced with unidirectional dry fibers using the hand lay-up (HLU) technique. The mixing ratio by weight of the resin and the fibers was 100:33, as recommended by the resin manufacturer.

The curing process consists of two phases. Initially, each specimen was placed inside a vacuum bag with breather assemblies. Air was extracted from the material using a vacuum pump and cure occurred at a controlled room temperature of 20°C. This vacuum bagging process consolidates the plies and significantly reduces voids in the composite material. After 24 h in room temperature, each specimen went through a secondary post-cure, during which the specimen is kept inside a furnace for 8 h at 60°C. Five specimens with 10 plies were produced. The number of plies and fiber orientations of each specimen, P1 to P5, are presented in Table 4.

These plies of either carbon fiber or glass fiber reinforced polymer composites may be considered transversely isotropic materials, as a result of their microscopic heterogeneity. It is therefore necessary to identify at least five independent elastic properties to characterize the behavior of the homogenized composite plies.[27] One of the main difficulties encountered in the computation simulation of the hybrid composites is the determination of these properties for each specimen

Table 1. Matrix components and properties.

Epoxy resin SR 1500 + Curing agent SD 2503	
Young's modulus (GPa)	2.86
Tensile strength (MPa)	71
Density (g/cm^3)	1.00
Poisson's ratio	0.3

Table 2. Mechanical and acoustic properties of the specimens.

Property	HS carbon	E-glass
Type of fabric	T700S	12.600
Fabric aerial weight (g/m^2)	225	600
Filament diameter (μm)	7	17
Filament maximum elongation	2.1%	4.8%
Filament Young's modulus (GPa)	230	74
Filament tensile strength (MPa)	4900	2500
Filament density (g/cm^3)	1.80	2.54
Filament Poisson's ratio	0.25	0.3

Table 3. Fiber volume fraction of hybrid composites and ply and laminate thickness.

Parameter	Values
Thickness of a carbon layer	0.24 mm
Thickness of a glass layer	0.43 mm
Total specimen thickness	3.16 mm
Carbon density	0.5071
Glass fraction	0.5860

Table 4. Material stacking sequences and ply fiber orientations of specimens made with carbon fiber (C) and glass fiber (G) reinforcements.

Specimen	Number of plies	Material stacking sequence	Ply fiber orientations
P1	10	$[C_3/G_2]_s$	$[0_3/90_2]_s$
P2			$[0_2/90_2/0]_s$
P3			$[0_4/90]_s$
P4			$[0_2/90_3]_s$
P5			$[0/90/0/90_2]_s$

Table 5. Properties of ply materials.

Ply material property		Carbon fiber	Glass fiber
Longitudinal tensile modulus	E_{11}	117.84 GPa	44.49 GPa
Transverse tensile modulus	E_{22}	9.73 GPa	11.34 GPa
In-plane Poisson's ratio	ν_{12}	0.27	0.30
Transverse Poisson's ratio	ν_{23}	0.25	0.23
In-plane Shear modulus	$G_{12} = G_{13}$	3.34 GPa	3.89 GPa
Transverse Shear modulus	G_{23}	2.40 GPa	2.78 GPa
Longitudinal tensile strength	X_T	2231 MPa	1100 MPa
Longitudinal compressive strength	X_C	1082 MPa	675 MPa
Transverse tensile strength	Y_T	29 MPa	35 MPa
Transverse compressive strength	Y_C	100 MPa	120 MPa
In-plane shear strength	$S_{12}=S_{13}$	60 MPa	80 MPa
Transverse shear strength	S_{23}	32 MPa	46 MPa

ply materials. To calculate the elastic properties it was first necessary to find the fiber volume ratio for each of them. Hence, two additional specimens were produced, one with only carbon fiber and another with only glass fiber plies both orientated at 0°. The total mass of the plies was measured before starting the HLU and both composites were weighted after the post-cure process to calculate the fiber volume ratio for the carbon fiber and the glass fiber composites. The fiber volume ratios obtained for the carbon fiber and glass fiber were the following: $v_{cf} = 0.5071$ and $v_{gf} = 0.5860$.

With the fiber volume ratios for each material and the data of Tables 1 and 2, it was finally possible to calculate the elastic properties for each specimen material layer, with the numerical method proposed and developed by Guedes and Kikuchi[28]: PREMAT. This finite element model is based on a homogenization theory, which assumes that the composite material is locally formed by the spatial repetition of very small microstructures called representative elementary volumes (RVE). Theoretically, it is mechanically admissible to use the elastic properties given by the periodic homogenization theory of this model due to the relative dimensions of the filament diameter compared to the thickness of each ply.[29] The elastic properties, obtained using this method, are presented in Table 5. The material strength of each ply used in the failure analysis was also obtained by the homogenization theory[28] (Table 5).

Experimental methods

Two types of experimental tests were performed, and deformations were measured for each specimen, subjected to bending–torsion loading. The constraints and the loading location in each experimental setup test are illustrated in Figure 1.

The experimental tests were conducted in Delft Aerospace Structures and Materials Laboratory at Delft University of Technology. Loading occurs at a rate of 2 mm/min and out-of-plane displacements are registered using a mechanical clip gauge in the vertical direction of the load location. A picture of each experimental setup is shown in Figure 2.

Experimental results

The experimental results are presented in Table 6. The out-of-plane displacement values were taken at the pin located in the corner of the specimen (applied load location – see Figure 1) for a loading of 50 N. This load has been selected to ensure that the specimen is kept within the linear elastic range and prior to any damage initiation.

With the coordinate system of Figure 1 and the data in Table 4, the influence of the fiber orientation of the plies is first analyzed, since all specimens have the same material distribution. By comparing the slope of the graphs in Figure 3, it can be observed that the number of plies at 0° and 90° fiber orientations in each specimen is extremely important for the displacement values. It can be easily seen that for the one side fixed experimental tests the most requested fibers are at 0°, whereas in the experimental test with two sides fixed, the most requested fibers are at 90°.

Numerical simulations by finite element analysis

A parametric finite element model of hybrid composite plates was developed using ABAQUS®. With the developed parametric model, it is possible to analyze plates with different plies orientation. This parametric model is very useful for the optimization process. In the finite

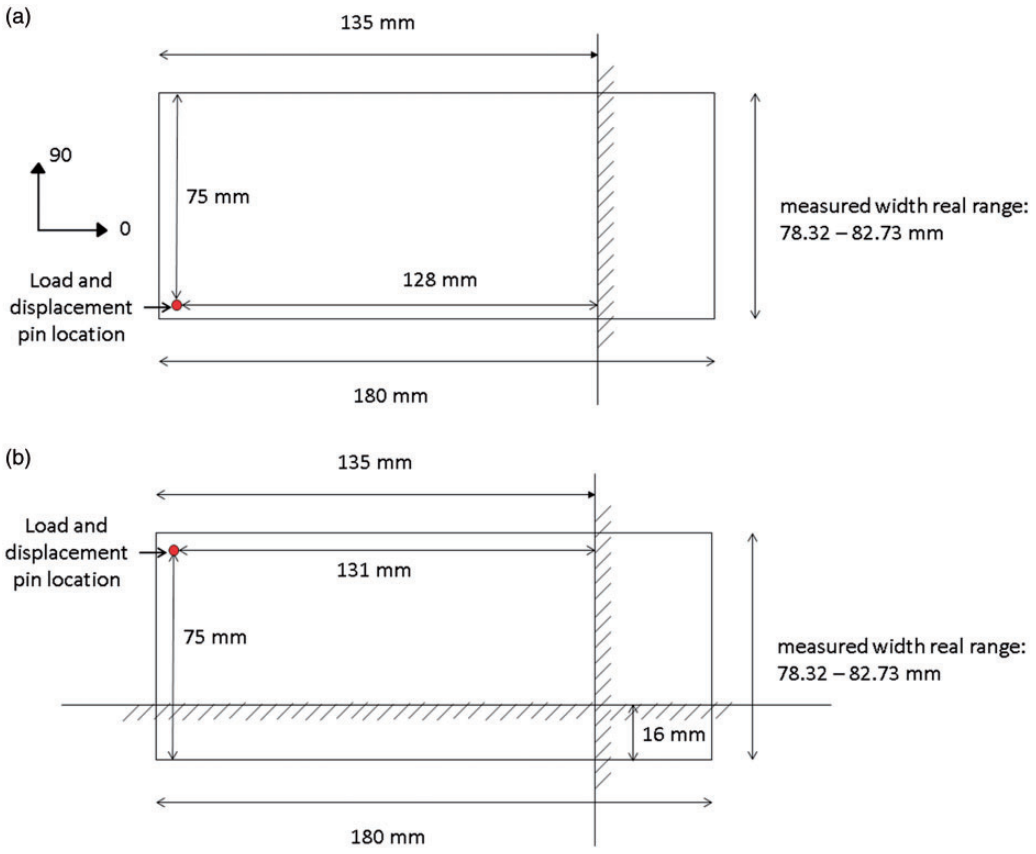

Figure 1. Illustration of the conducted experimental setup tests: (a) plate fixed in one side and (b) plate fixed in two sides.

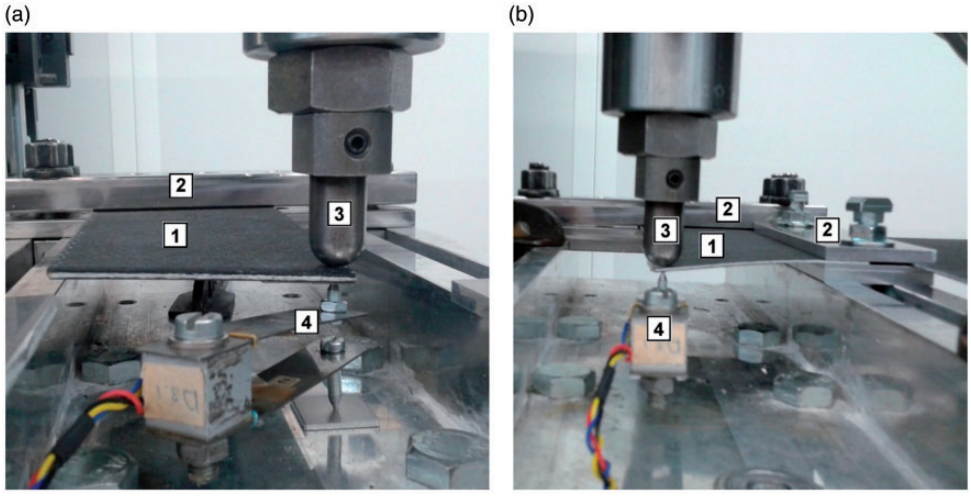

Figure 2. Experimental bending–torsion tests with the hybrid composite plates: (a) one side fixed; (b) two sides fixed. 1 – plate; 2 – fixed side; 3 – load application; 4 – mechanical clip gauge.

element analysis (FEA), all five plates presented in Table 4 were numerically simulated in order to validate the numerical results with the experimental out-of-plane displacements presented in Table 6. A failure analysis was performed based on the FEA results using Hashin's failure criteria[30,31] for all plates in order to ensure that the 50 N load is within the linear elastic domain and prior to any damage initiation.

Table 6. Out-of-plane displacements obtained in experimental tests for different loading values.

Specimen	Material stacking sequence	Ply fiber orientations	Experimental test	Loading (N)	Experimental displacement (mm)
P1	$[C_3/G_2]_s$	$[0_3/90_2]_s$	One side fixed	50	3.71
P2		$[0_2/90_2/0]_s$			3.89
P3		$[0_4/90]_s$			3.49
P4		$[0_2/90_3]_s$			4.40
P5		$[0/90/0/90_2]_s$			4.33
P1	$[C_3/G_2]_s$	$[0_3/90_2]_s$	Two sides fixed	50	1.69
P2		$[0_2/90_2/0]_s$			1.37
P3		$[0_4/90]_s$			2.40
P4		$[0_2/90_3]_s$			1.26
P5		$[0/90/0/90_2]_s$			1.16

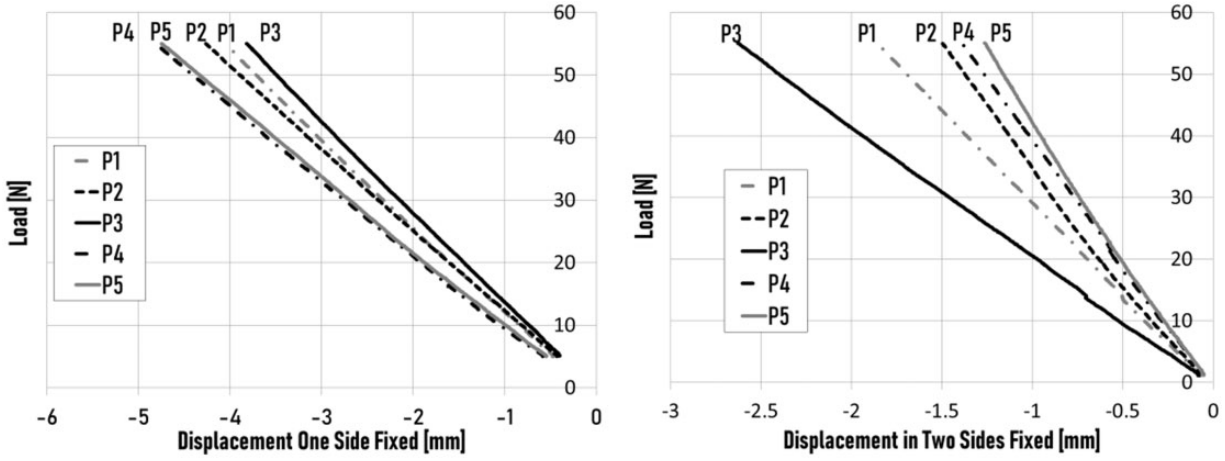

Figure 3. Load–displacement results obtained in the experimental tests.

Plies elastic properties considered for the laminates are shown in Table 5, which were obtained with the aforementioned homogenization method. For each experimental setup (one side fixed and two sides fixed), two models were built: one using a four-node linear shell element (S4) and another one using an eight-node quadratic shell element (S8). A convergence test was done for all five plates for both boundary conditions. The P5 plate with one side fixed has the higher displacement value and also has the slower convergence curve as is shown in Table 7. So, after the convergence test, a significant number of elements was used to avoid any loss of precision in the optimization method. The same number of elements was used for S4 and S8 shell elements. Specifically, depending on the experimental setup, 3844 and 3224 elements were used, for one side fixed and two sides fixed, respectively. Computational displacement was measured at the load point, as depicted in Figure 4.

FEA numerical results

Table 8 presents the out-of-plane displacements obtained using the FEA as well as the corresponding experimental values. The first immediate observation is that the displacement obtained from the linear and quadratic shell element models are almost equal. Therefore, the linear four-node shell element proves to be sufficient for the optimization process while enabling a faster process. Comparing experimental with numerical results, the discrepancy for the one side fixed plates is smaller than for the two sided fixed plates. For all cases, the measured displacement in the experiments is larger than the displacement obtained by FEA. This has also been observed in previous works found in literature, where the flexural stiffness measured in the experiments was lower than the one predicted by the numerical and analytical models.[3,4] The discrepancy is most probably related with the degree of

Table 7. Convergence test considering P5 with one fixed side.

	S4 element		S8 element	
Number of elements	Computational displacement (mm)	Maximum σ_{11} (MPa)	Computational displacement (mm)	Maximum σ_{11} (MPa)
704	3.93	154.5	3.94	156.8
1344	3.93	154.5	3.94	156.8
1924	3.94	154.5	3.94	156.8
2184	3.94	154.5	3.94	156.8
3244	3.94	154.5	3.94	156.8
3844	3.94	154.5	3.94	156.8
4154	3.94	154.5	3.94	156.8

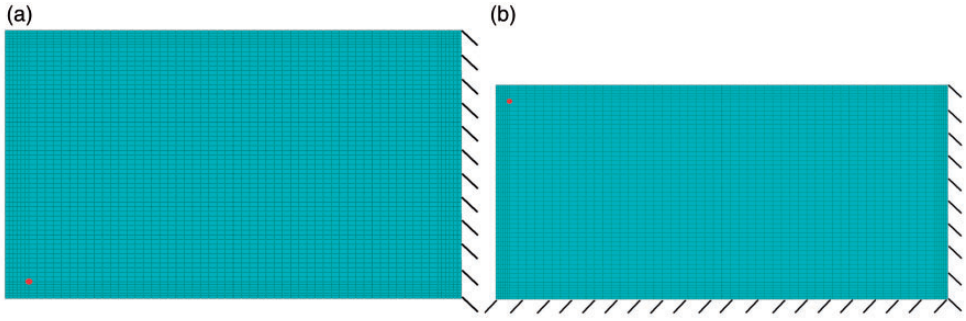

Figure 4. Mesh, boundary conditions, and load/computational displacement point in red: (a) one side fixed and (b) two sides fixed.

Table 8. Out-of-plane displacements and discrepancy percentage between the experimental and the computational analysis using the four-node element.

Specimen	Experimental test	Experimental displacement (mm)	Computational displacement (4 nodes) (mm)	Computational displacement (8 nodes) (mm)	Δ %	Hashin's fiber initiation criterion	Hashin's matrix initiation criterion
P1	One side fixed	3.71	3.12	3.12	15.9	0.0028	0.0233
P2		3.89	3.57	3.56	8.2	0.0038	0.0124
P3		3.49	3.04	3.04	12.9	0.0027	0.0343
P4		4.40	3.58	3.58	18.6	0.0039	0.0123
P5		4.33	3.94	3.94	9.0	0.0048	0.0142
P1	Two sides fixed	1.69	1.43	1.43	15.4	0.0004	0.4655
P2		1.37	0.91	0.91	33.3	0.0002	0.1785
P3		2.40	1.70	1.70	29.2	0.0007	0.6909
P4		1.26	0.91	0.90	28.2	0.0002	0.1741
P5		1.16	0.77	0.77	33.6	0.0002	0.1255

fixation stiffness at the boundary conditions. In theory, fixed constraints do not allow any displacement or rotation, which is in fact numerically simulated in the model. However, on the actual experimental test, absolute zero displacements and rotations are very difficult to assure and small displacement and rotations probably occur in fixed sides. Hence, for two sides fixed plates the difference between experimental and computational analysis is naturally higher. In order to better replicate the experimental conditions, fixed constraints that allow infinitesimal rotations were considered (i.e. partially fixed). Boundary conditions were

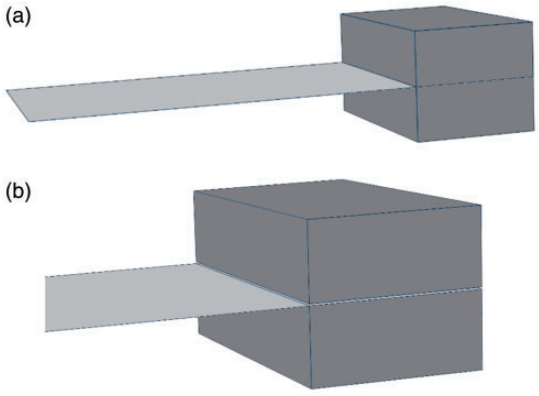

Figure 5. (a) One side totally fixed and (b) One side partially fixed (gap was increased 100 times for visualization purposes).

simulated with standard eight-node elements for steel grips. Contrary to fixed conditions, for which there is no gap between steel grips and plate (Figure 5(a)), for partially fixed conditions, a 5 μm gap is used between top grip and plate, allowing a maximum rotation of 0.1° (Figure 5(b)). The results of this adapted model are shown in Table 9. As expected, the discrepancy between the model and experiments is now smaller, but some differences still persist. This might be related with the ply properties assumed in the model, which depend on thickness, and the fact that a perfect homogenized ply is almost impossible to manufacture. Figure 6 shows plots of the out-of-plane displacement field from the FEAs with totally and partially fixed rotation.

Table 9. Out-of-plane displacements and discrepancy percentage between the experimental and the computational analysis using partially fixed rotation (instead of totally fixed).

Specimen	Experimental test	Experimental displacement (mm)	Totally fixed (mm)	Partially fixed (mm)	Δ %
P1	One side fixed	3.71	3.12	3.50	5.7
P2		3.89	3.57	3.95	−1.5
P3		3.49	3.04	3.43	1.7
P4		4.40	3.58	3.97	9.8
P5		4.33	3.94	4.32	0.2
P1	Two sides fixed	1.69	1.43	1.67	1.2
P2		1.37	0.91	1.13	17.5
P3		2.40	1.70	1.96	18.3
P4		1.26	0.91	1.12	11.1
P5		1.16	0.77	0.98	15.7

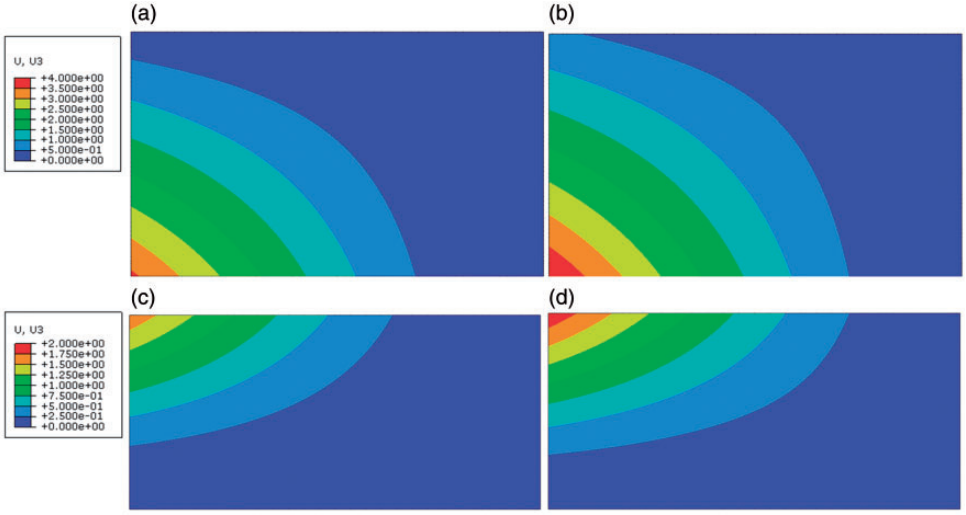

Figure 6. Displacements in mm: (a,b) P1 with one side fixed; (c,d) P1 with two sides fixed; (b,d) with partially fixed rotations.

Table 10. Optimal solutions obtained by GLODS for each experimental setup, with two local minima for the case of plate fixed in two sides.

Specimen	Experimental test	Number of plies	Material stacking sequence	Ply fiber orientations	Displacement value (mm)
P6	One side fixed	10	$[C_3/G_2]_s$	[15/15/15/0/15]s	2.130
P7	Two side fixed			[−60/90/−60/60/−45]s	0.358
P8	Two side fixed			$[-60/-60/75/-60/-60]_s$	0.357

Table 11. Out-of-plane displacements results of the optimized specimens P6, P7, and P8.

Specimen	Experimental displacement (mm)	Computational displacement – totally fixed (mm)	Computational displacement – partially fixed (mm)
P6	2.35	2.130	2.420
P7	0.60	0.358	0.576
P8	0.62	0.357	0.582

Table 8 also presents the results for Hashin's fiber and matrix failure initiation criterion. For both fiber and matrix criteria, Table 8 only shows the highest value, which is in all cases the tensile one. As is possible to observe all plates (one sided and two sided fixed) have Hashin's criterion values below 1, which means that no failure occurs.

Optimization

The optimization of the specimens was carried out using GLODS, a single objective global optimization method that uses an efficient multistart strategy. The objective function is focused on the minimization of the maximum out-of-plane displacement value. The objective function evaluation is made through an FEA software ABAQUS®. For clarity, a brief introduction to GLODS is given followed by the optimization method used in order to introduce the optimization problem solved and present the optimal results.

GLODS method

A constrained nonlinear optimization problem can be mathematically formulated as:

Find $\boldsymbol{n}$ design variables

$$\mathbf{x} = (x_1, x_2, \ldots, x_n)^{\mathrm{T}} \in \boldsymbol{\Omega} \subseteq \mathbb{R}^n \tag{1}$$

which minimize

$$\min_{\mathbf{x} \in \boldsymbol{\Omega}} f(\mathbf{x}) \tag{2}$$

where $f: \boldsymbol{\Omega} \subseteq \mathbb{R}^n \rightarrow \mathbb{R} \cup \{+\infty\}$ represents the real-extended value function and $\boldsymbol{\Omega} \subseteq \mathbb{R}^n$ represents the compact set, defining the problem feasible region.

GLODS[32] is a solver suited for global constrained single optimization, which does not use any derivatives of the objective functions.

Using direct search of directional type, the method alternates between a search step, where potentially good regions are located, and a poll step, where the previously located regions are explored. This exploration is made through the launching of several pattern search methods, one in each of the regions of interest. Differently from a multistart strategy, the several pattern search methods will merge when sufficiently close to each other. The goal of GLODS algorithm is to end with as many active pattern searches as the number of local minimizers, which would allow locating easily the possible global extreme value. Similarly to other derivative-free optimization algorithms, it makes use of the extreme barrier function $f_{\boldsymbol{\Omega}}(\mathbf{x})$ defined as

$$f_{\boldsymbol{\Omega}}(\mathbf{x}) = \begin{cases} f(\mathbf{x}) & \text{if } \mathbf{x} \in \boldsymbol{\Omega} \\ +\infty & \text{otherwise} \end{cases} \tag{3}$$

Unfeasible points will not be evaluated, being the corresponding objective function value set equal to $+\infty$. This approach allows dealing with black-box type constraints, where only a yes/no type of answer is returned. Several details are omitted in the present text and the reader is referred to Custodio and Madeira[32] for a more complete description.

Optimal design formulation

In this work, the objective function is to minimize the maximum out-of-plane displacement in a composite specimen made with 10 layers with symmetric material stacking sequence $[C_3/G_2]_s$, where C stands for carbon fiber and G for glass fiber. The evaluation of the objective function is made through an FEA software, ABAQUS®.

The design variables are the angles of the fiber orientation of five plies of the symmetric stacking sequence $[C_3/G_2]_s$ indicated as

$$\mathbf{x} = (x_1, x_2, x_3, x_4, x_5)^{\mathrm{T}} \tag{4}$$

These angles are discrete variables with allowable variation of 5° in the domain

$$-85^\circ \leq x_i \leq 90^\circ, i = 1, \ldots, 5 \tag{5}$$

In the optimization process, the default parameters of GLODS are used and the local minimums are found (after 10,000 evaluations of the objective function) for each experimental setup: (a) plate fixed in one side and (b) plate fixed in two sides. The optimization carried out considered in the ABAQUS® simulations the theoretical fixed displacement and rotation as boundary conditions (i.e. totally fixed). These optimal results are presented in Table 10 for both experimental setups. The Hashin's failure criteria were also applied to the three optimized stacking sequences. For the optimized plates, the highest value for the Hashin's fiber criterion is 0.0027 for specimen P6 and for the Hashin's matrix criterion is 0.0148 for specimen P8. Both values are below one, which means that no failure is expected in the optimized plates for the tested load.

Experimental validation of the optimized laminates

Once the optimized stacking sequence of ply fiber orientations is obtained, it is important to validate the optimization process by performing experimental tests on the proposed optimized solutions. For experimental validation, the three optimized specimen configurations (P6, P7, and P8 of Table 10) obtained in the optimization process were manufactured using the same technique as the previous specimens P1, P2, P3, P4, and P5.

Table 11 presents the experimental and numeric results of the out-of-plane displacement at the location of the applied load, including the numerical results for both cases of totally and partially fixed rotation boundary conditions.

Figures 7 and 8 compare the out-of-plane displacement results for the non-optimized specimens (P1, P2, P3, P4, and P5) against the optimized specimens (P6, P7, and P8) considering the one side fixed condition and the two sides fixed condition, respectively.

It is quite clear from Figures 7 and 8 the significant decrease of the out-of-plane displacement of the

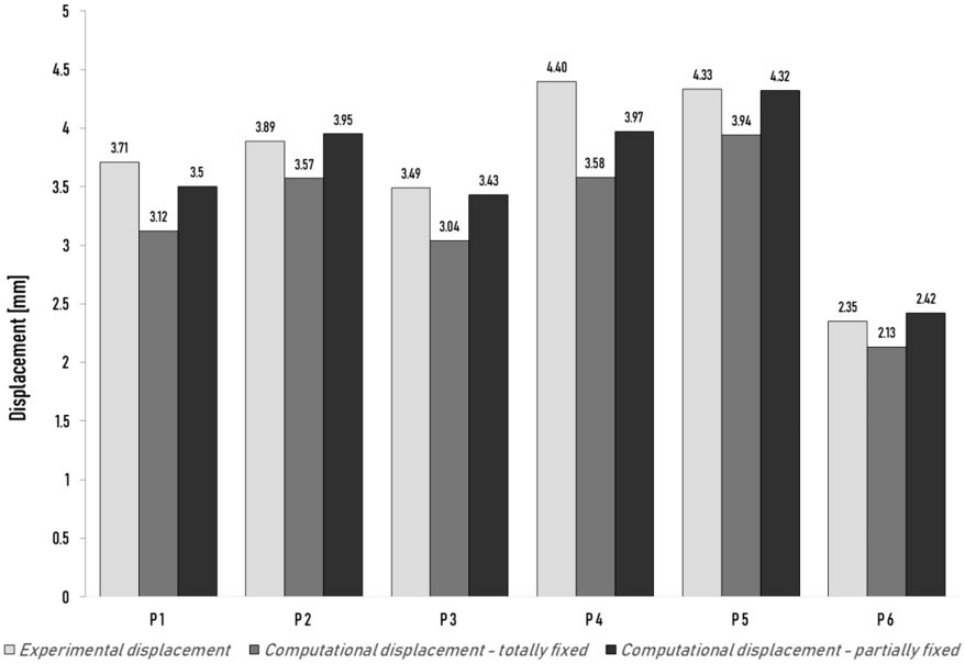

Figure 7. Comparison of experimental and computational values obtained for the non-optimized specimens (P1, P2, P3, P4, and P5) and the optimized specimens (P6) considering the plate fixed in one side.

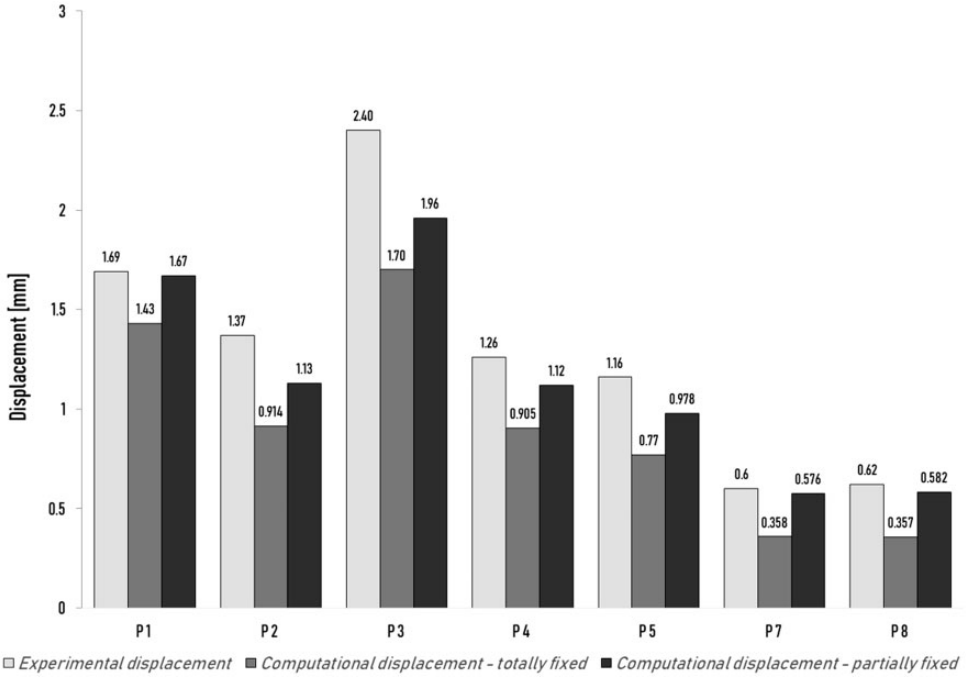

Figure 8. Comparison of experimental and computational values obtained for the non-optimized specimens (P1, P2, P3, P4, and P5) and the optimized specimens (P7 and P8) considering the plate fixed in two sides.

optimized specimens found by GLODS, P6, P7, and P8, when compared to the non-optimized specimens, P1, P2, P3, P4, and P5, for both sets of boundary conditions. This decrease in out-of-plane displacement from non-optimized laminates to optimized laminates is in accordance with previous optimization works using GLODS with 100% carbon fiber reinforced laminates under combined loading bending and torsion.[26]

It is important to recognize that experimental measurements are considered to be the true deformation of the composite specimens, although in reality experimental errors may be inherently present. Specifically, the manufacturing process of each sample may introduce a few unforeseeable imperfections,[26,33] since the laminate quality in HLU is very dependent on the skills of the producer, just as the curing process and the final cutting of the specimen. Meanwhile, the thickness of each carbon fiber ply and each glass fiber ply was calculated with mean values of measurements of the carbon fiber and glass fiber laminates, respectively. Each of the five specimens was measured in nine points and it was verified that the estimated thickness of the carbon fiber and glass fiber plies had a very good approximation. However, the fact that these values were taken into account in the development of the finite element models may also have contributed to some deviations in the computational results. Additionally, the calculation of the elastic properties of the carbon fiber and glass fiber plies was done by a numerical method based on a homogenization theory. This method depends on the definition of geometric parameters of the representative elementary volume, and as such, it is possible that small errors are associated with these properties relatively to the ply material properties of the specimens tested in the experiments.

The inherent uncertainties altogether, namely, the specimens manufacture using HLU, the real ply material properties, and the complexity of replicating numerically the exact boundary conditions placed in the experimental setup tests, naturally introduce some small expected discrepancy between the experimental and computational results. Even so, the optimization process is shown to be quite successful. Not only the computational results of the optimized specimens are validated by the experimental tests (within a reasonable discrepancy) but also the desired improvement of the performance of the hybrid composite plates is achieved in more than 30% when compared to some non-optimized plates. Furthermore, an important aspect that is demonstrated by the optimization of these hybrid carbon–glass epoxy composites is that the most common ply fiber orientations of 0°, 90°, and even $\pm 45^\circ$ adopted for various laminated composite applications rather limits somewhat their performance. In a real combined loading condition of bending and torsion, different ply fiber orientations should be explored in the interest of maximizing the hybrid laminated composite performance. This has also been observed for single fiber laminates.[26]

Conclusions

The increasing relevance of hybrid carbon–glass epoxy composites, whose mechanical properties can be tailored to take advantage of the better properties of both fiber types, relies on their potential for an increased performance compared to standard composites using one type of fiber alone. The aim of this work was to optimize the hybrid composite stacking sequence, using the ply fiber orientation as design variable to minimize the maximum out-of-plane displacement under combined loading of bending and torsion. In order to study normal operation conditions, a load within the material linear elastic domain and prior to any damage initiation was considered, as verified throughout the experimental tests and the results from the Hashin's failure criteria.

The optimization process is shown to be quite successful, contributing to improve the performance of the hybrid composite plates in more than 30% when compared to some non-optimized plates. In addition, it is shown that ply fiber orientations different to the most usual 0°, 90°, and ±45° should be explored in the interest of maximizing the hybrid laminated composite performance under combined loading of bending and torsion.

Declaration of Conflicting Interests

The author(s) declared no potential conflicts of interest with respect to the research, authorship, and/or publication of this article.

Funding

The author(s) disclosed receipt of the following financial support for the research, authorship, and/or publication of this article: This work was supported by "Fundação para a Ciência e a Tecnologia" (FCT), through the Institute of Mechanical Engineering (IDMEC) under the Associated Laboratory for Energy, Transports and Aeronautics (LAETA), Project UID/EMS/50022/2019, and by the Netherlands Organisation for Scientific Research (NWO), project number 14366.

ORCID iD

Rui B Ruben http://orcid.org/0000-0002-5407-0579
F Moleiro http://orcid.org/0000-0001-9287-3519
Sofia Teixeira de Freitas http://orcid.org/0000-0002-0847-6287

References

1. Pandya KS, Veerraju C and Naik NK. Hybrid composites made of carbon and glass woven fabrics under quasi-static loading. *Mater Des* 2011; 32: 4094–4099.
2. Enfedaque A, Molina-Aldareguía JM, Gálvez F, et al. Effect of glass fiber hybridization on the behavior under impact of woven carbon fiber/epoxy laminates. *J Compos Mater* 2010; 44: 3051–3068.
3. Dong C, Ranaweera-Jayawardena HA and Davies IJ. Flexural properties of hybrid composites reinforced by S-2 glass and T700S carbon fibres. *Compos B Eng* 2012; 43: 573–581.
4. Dong C and Davies IJ. Flexural strength of bidirectional hybrid epoxy composites reinforced by E glass and T700S carbon fibres. *Compos B Eng* 2015; 72: 65–71.
5. Kretsis G. A review of the tensile, compressive, flexural and shear properties of hybrid fibre-reinforced plastics. *Composites* 1987; 18: 13–23.
6. Naik NK, Ramasimha R, Arya H, et al. Impact response and damage tolerance characteristics of glass-carbon/epoxy hybrid composite plates. *Compos B Eng* 2001; 32: 565–574.
7. Hosur MV, Adbullah M and Jeelani S. Studies on the low-velocity impact response of woven hybrid composites. *Compos Struct* 2005; 67: 253–262.
8. Sayer M, Bektaş NB, Demir E, et al. The effect of temperatures on hybrid composite laminates under impact loading. *Compos B Eng* 2012; 43: 2152–2160.
9. González EV, Maimí P, Sainz de Aja JR, et al. Effects of interply hybridization on the damage resistance and tolerance of composite laminates. *Compos Struct* 2014; 108: 319–331.
10. Zhang J, Chaisombat K, He S, et al. Hybrid composite laminates reinforced with glass/carbon woven fabrics for lightweight load bearing structures. *Mater Des* 2012; 36: 75–80.
11. Dong C and Davies IJ. Optimal design for the flexural behaviour of glass and carbon fibre reinforced polymer hybrid composites. *Mater Des* 2012; 37: 450–457.
12. Dong C and Davies IJ. Flexural and tensile strengths of unidirectional hybrid epoxy composites reinforced by S-2 glass and T700S carbon fibre. *Mater Des* 2014; 54: 955–966.
13. Kalantari M, Dong C and Davies IJ. Multi-objective analysis for optimal and robust design of unidirectional glass/carbon fibre reinforced hybrid epoxy composites under flexural loading. *Compos B Eng* 2016; 84: 130–139.
14. Kalantari M, Dong C and Davies IJ. Multi-objective robust optimisation of unidirectional carbon/glass fibre reinforced hybrid composites under flexural loading. *Compos Struct* 2016; 138: 264–275.
15. Swolfs Y, Gorbatikh L and Verpoest I. Fibre hybridisation in polymer composites: a review. *Composites Part A* 2014; 67: 181–200.
16. Gurdal Z, Haftka RT and Hajela P. *Design and optimization of laminated composite materials*. New York: Wiley-Interscience, 1999.
17. Todoroki A and Haftka RT. Stacking sequence optimization by a genetic algorithm with a new recessive gene like repair strategy. *Compos Part B* 1998; 29: 277–285.
18. Toropov VV, Jones R, Willment T, et al. Weight and manufacturability optimization of composite aircraft components based on a genetic algorithm. In: *6th world congress of structural and multidisciplinary optimization*, Rio de Janeiro, Brazil, 30 May–3 June 2005.
19. Zhu X, He R, Lu X, et al. A optimization technique for the composite strut using genetic algorithms. *Mater Des* 2015; 65: 482–488.

20. Ghiasi H, Pasini D and Lessard L. Optimum stacking sequence design of composite materials part I: constant stiffness design. *Compos Struct* 2009; 90: 1–11.
21. Custodio AL, Madeira JFA, Vaz AIF, et al. Direct multisearch for multiobjective optimization. *SIAM J Optim* 2011; 21: 1109–1140.
22. Araújo AL, Madeira JFA, Mota Soares CM, et al. Optimal design for active damping in sandwich structures using the Direct MultiSearch method. *Compos Struct* 2013; 105: 29–34.
23. Madeira JFA, Araújo AL, Mota Soares CM, et al. Multiobjective design of viscoelastic laminated composite sandwich panels. *Compos B Eng* 2015; 77: 391–401.
24. Madeira JFA, Araújo AL, Mota Soares CM, et al. Multiobjective optimization of viscoelastic laminated sandwich structures using the Direct MultiSearch method. *Compos Struct* 2015; 147: 229–235.
25. Franco Correia VM, Madeira JA, Araújo AL, et al. Multiobjective design optimization of laminated composite plates with piezoelectric layers. *Compos Struct* 2017; 169: 10–20.
26. Monte SMC, Infante V, Madeira JFA, et al. Optimization of fibers orientation in a composite specimen. *Mech Adv Mater Struct* 2017; 24: 410–416.
27. Melro AR, Camanho PP and Pinho ST. Influence of geometrical parameters on the elastic response of unidirectional composite materials. *Compos Struct* 2012; 94: 3223–3231.
28. Guedes J and Kikuchi N. Preprocessing and postprocessing for materials based on the homogenization method with adaptive finite element methods. *Comput Meth Appl Mech Eng* 1990; 83: 143–198.
29. Coelho PG, Amiano LD, Guedes JM, et al. Scale-size effects analysis of optimal periodic material microstructures designed by the inverse homogenization method. *Comput Struct* 2015; 174: 21–32.
30. Hashin Z. Failure criteria for unidirectional fiber composites. *J Appl Mech* 1980; 47: 329–334.
31. Kress G. Examination of Hashin's failure criteria for Part B of the second world-wide failure exercise: comparison with test data. *J Compos Mater* 2013; 47: 867–891.
32. Custodio AL and Madeira JFA. GLODS: global and local optimization using direct search. *J Global Optim* 2015; 62: 1–28.
33. Hucker MJ, Bond IP, Haq S, et al. Influence of manufacturing parameters on the tensile strengths of hollow and solid glass fibres. *J Mater Sci* 2002; 37: 309–315.